Taking a look into the orbit of mammalian carnivorans

Carlos Casares-Hidalgo,[1] Alejandro Pérez-Ramos,[1] Manuel Forner-Gumbau,[2] Francisco J. Pastor[3] and Borja Figueirido[1]

[1]Departamento de Ecología y Geología, Facultad de Ciencias, Universidad de Málaga, Málaga, Spain
[2]Departament de Matemàtiques, Facultat de Ciències, Universitat Jaume I (Castelló de la Plana), Castellón de la Plana, Spain
[3]Departmento de Anatomía y Radiología, Museo de Anatomía, Universidad de Valladolid, Valladolid, Spain

Abstract

In this study, we explore the relationship between orbit anatomy and different ecological factors in carnivorous mammals from a phylogenetic perspective. We calculated the frontation (α), convergence (β), and orbitotemporal (Ω) angles of the orbit from 3D coordinates of anatomical landmarks in a wide sample of carnivores with different kinds of visual strategy (i.e. photopic, scotopic, and mesopic), habitat (i.e. open, mixed, and closed), and substrate use (i.e. arboreal, terrestrial, and aquatic). We used Bloomberg's *K* and Pagel's λ to assess phylogenetic signal in frontation, convergence, and orbitotemporal angles. The association of orbit orientation with skull length and ecology was explored using phylogenetic generalized least squares and phylogenetic MANOVA, respectively. Moreover, we also computed phylomorphospaces from orbit orientation. Our results indicate that there is not a clear association between orbit orientation and the ecology of living carnivorans. We hypothesize that the evolution of the orbit in mammalian carnivores represents a new case of an ecological bottleneck specific to carnivorans. New directions for future research are discussed in light of this new evidence.

Key words: habitat use; mammalian carnivores; orbit anatomy; phylogenetic signal; visual strategy.

Introduction

Orbit (eye socket; Fig. 1A) orientation is an important eco-morphological indicator in vertebrates due to its visual implications (e.g. Cartmill, 1970, 1974, 2017). Animals with more lateral orbits exhibit high panoramic vision (or monocular vision) with little or no overlap among visual fields. Monocular vision has been studied across different prey species, such as artiodactyls, equids, and lagomorphs, and a strong relationship has been established between orbit lateralization and fast detection of predators (e.g. Walls, 1942; Hughes, 1977). In contrast, species with forward-facing orbits exhibit low panoramic vision with substantial overlap among visual fields (or binocular vision). Binocular vision has the advantages of more light capture, better depth perception, and better contrast, which provide several visual advantages for active predation (e.g. Pirenne, 1943; Campbell & Green, 1965; Hughes, 1977; Garamszegi et al. 2002; Heesy, 2004, 2008). Additionally, binocular vision provides the ability to detect an object when something is obstructing the view by the overlap of the same visual information extracted from similar images presented to each eye (e.g. Allman, 1977; Cartmill, 2017). Therefore, binocular vision is typical of predatory behaviour because it allows stereoscopic depth perception (e.g. Heesy, 2008). For this reason, orbit anatomy has been used to decipher visual abilities in a plethora of extinct taxa including early tetrapods (MacIver et al. 2017), non-mammalian synapsids (Angielczyk & Schmitz, 2014), dinosaurs (Schmitz & Motani, 2011), and ichthyosaurs (Motani et al. 1999).

Previous researchers have demonstrated that specific angles of the orbit in mammals are associated with substrate use (e.g. Cartmill, 1974) or with circadian activity pattern (e.g. Crompton, 1995). Despite the fact that locomotion in a complex arboreal environment does not require binocular vision (Cartmill, 1974, 1992, 2017), arboreal taxa show the highest level of orbit convergence among mammals (Heesy, 2008). Moreover, as more convergent orbits have larger zones of binocular visual field overlap, and scales similarly across mammalian orders (Heesy, 2004), orbit orientation is a good proxy for binocular visual field overlap.

Previous studies have demonstrated that 45% of orbit orientation variance in mammals is explained by ecological factors such as activity pattern, substrate preference, and the degree of faunivory (Heesy, 2008). The same analyses performed solely in non-primate eutherian mammals
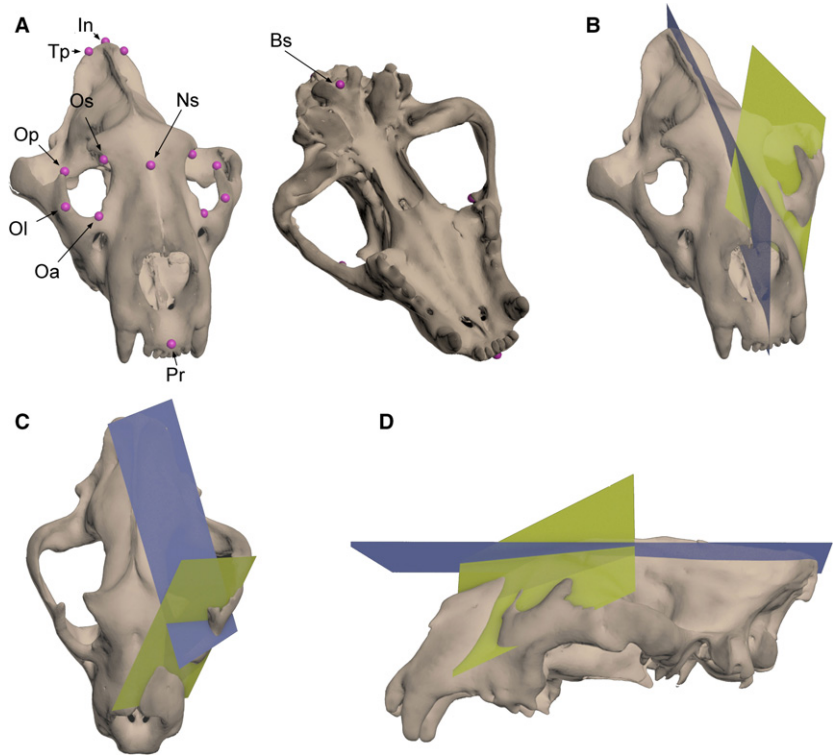
Fig. 1 Calculation of orbit orientation in carnivores. (A) Anatomical landmarks in three dimensions used to define the planes to analyse the orientation of the orbit: Op (orbitale posterius), most posterior point of the orbit; Oa (orbitale anterius), most anterior point of the orbit; Ol (orbitale lateralis), most lateral point of the orbit; Os (orbitale superius), highest point of the orbit; Tp, most posterior point of the temporal fossa; Pr, prostion; Ns, nasion; In, inion; Bs, basion. (B) Convergence angle (β) measured as the dihedral angle between the sagittal plane (blue) and the orbital plane (green). (C) Orbitotemporal angle (Ω) measured as the dihedral angle between the temporal plane (blue) and the orbital plane (green); (D) Frontation angle (α) measured as the dihedral angle between the dorsal plane (blue) and the orbital plane (green).

demonstrated that 44% of orbit orientation variance is explained by ecological factors. Other authors have also demonstrated a significant correlation between orbit orientation in mammals and the degree of canopy cover in the inhabited ecosystem (Changizi & Shimojo, 2008). All these studies have been performed using broad taxonomic samples with the main goal of finding general ecological patterns shaping orbit orientation and size across mammals. However, detailed studies focused on specific taxonomic groups with more refined ecological categories are less common.

In this article, we perform a detailed study on orbit orientation in the mammalian order Carnivora as a proxy for visual field overlap to explore the relationship between visual strategy and different ecological factors. Specifically, we characterize orbit orientation based on the frontation (α), convergence (β), and orbitotemporal (Ω) angles (e.g. Cartmill, 1970; Ravosa et al. 2000; Heesy, 2005), and we test the association of these angles with the type of vision (i.e. photopic, scotopic or mesopic), the vegetation structure of the inhabited ecosystem (i.e. closed, mixed or open habitats), and substrate preference (i.e. terrestrial, arboreal or aquatic) under a phylogenetic framework.

Our specific goals are (1) to explore whether orbit orientation is associated with the ecology of carnivores; (2) to test for the effect of skull length, i.e. allometric effects, on orbit orientation; (3) to investigate the influence of phylogeny on orbit orientation by mapping frontation, convergence, and orbitotemporal angles onto a carnivoran phylogenetic tree; and (4) to depict a phylomorphospace

for orbit orientation that allows the phylogenetic occupation of this morphospace to be reconstructed. Our hypothesis is that orbit orientation is correlated with the specific ecology of carnivorans, as previously demonstrated in other studies with a broader taxonomic range (e.g. Heesy, 2008).

Materials and methods

Taxa sampled

We collected 192 skulls of 107 species belonging to 13 families of living mammalian carnivores: Ailuridae (1), Canidae (20), Felidae (23), Hyaenidae (3), Ursidae (7), Mustelidae (13), Herpestidae (5), Viverridae (4), Eupleridae (3), Procyonidae (6), Phocidae (12), Otariidae (6), and Odobenidae (1) (see Table 1 and Fig. 2).

The skulls are housed in the collections of the Department of Anatomy at the University of Valladolid (Spain), Smithsonian National Museum of Natural History (USNM, Washington, DC, USA), American Museum of Natural History (AMNH, USA), National Museum of Scotland (NMS, UK) and the Museum für Naturkunde Berlin (MFN, Germany).

We collected only adult individuals, as indicated by closed basilar synchondroses and complete tooth eruption. We also included two sabre-tooths, *Smilodon fatalis* and *Homotherium serum* (collected from DigiMorph, http://digimorph.org/), as fossil species, without living analogues, adapted to deploy a specialized killing bite (Slater & Van Valkenburgh, 2008; Figueirido et al. 2010, 2018).

Orbit orientation

All the data were collected by A.P.-R. with a MicroScribe G2X by digitizing 14 three-dimensional landmarks (Fig. 1A) to define the

Table 1 Species of the order Carnivora included in the study with average values of frontation (Ω), convergence (β), and orbitotemporal (Ω) angles, as well as skull length (Sk. Length). The ecological classifications were established following the literature (see text for details).

Family	Specie	Activity	Habitat	Substrate	α (°)	β (°)	Ω (°)	Sk. Length (mm)
Ailuridae	*Ailurus fulgens*	Nocturnal	Closed	Arboreal	54.72	59.18	46.30	97.79
Canidae	*Canis aureus*	Nocturnal	Mixed	Terrestrial	58.55	44.46	37.46	146.78
Canidae	*Canis latrans*	Crepuscular	Mixed	Terrestrial	60.93	46.35	41.12	174.56
Canidae	*Canis lupus*	Crepuscular	Mixed	Terrestrial	60.51	46.04	41.80	213.53
Canidae	*Canis mesomelas*	Nocturnal	Opened	Terrestrial	57.58	45.85	39.02	143.40
Canidae	*Cerdocyon thous*	Nocturnal	Closed	Terrestrial	57.78	45.56	34.22	132.64
Canidae	*Chrysocyon brachyurus*	Nocturnal	Mixed	Terrestrial	65.97	46.06	39.51	194.33
Canidae	*Cuon alpinus*	Crepuscular	Mixed	Terrestrial	58.81	44.39	35.66	164.04
Canidae	*Lycalopex culpaeus*	Nocturnal	Opened	Terrestrial	52.72	50.48	37.54	144.56
Canidae	*Lycalopex gymnocercus*	Nocturnal	Opened	Terrestrial	51.76	50.53	32.75	118.58
Canidae	*Lycalopex vetulus*	Nocturnal	Mixed	Terrestrial	55.34	48.44	35.91	101.52
Canidae	*Lycaon pictus*	Crepuscular	Opened	Terrestrial	54.26	50.24	41.06	181.34
Canidae	*Nyctereutes procyonoides*	Nocturnal	Closed	Arboreal	56.51	49.16	37.49	107.82
Canidae	*Otocyon megalotis*	Crepuscular	Opened	Terrestrial	59.01	42.95	34.50	102.53
Canidae	*Speothos venaticus*	Diurnal	Closed	Terrestrial	53.66	50.01	34.24	123.53
Canidae	*Urocyon cinereoargenteus*	Nocturnal	Closed	Arboreal	66.15	41.93	40.86	106.80
Canidae	*Vulpes chama*	Nocturnal	Opened	Terrestrial	59.99	40.95	44.14	90.62
Canidae	*Vulpes lagopus*	Nocturnal	Opened	Terrestrial	54.89	45.37	34.24	123.10
Canidae	*Vulpes macrotis*	Nocturnal	Opened	Terrestrial	54.14	47.56	34.10	108.44
Canidae	*Vulpes velox*	Nocturnal	Opened	Terrestrial	55.05	45.58	34.93	103.34
Canidae	*Vulpes vulpes*	Nocturnalr	Mixed	Terrestrial	51.66	49.20	34.08	140.85
Canidae	*Vulpes zerda*	Nocturnal	Opened	Terrestrial	56.32	45.84	35.38	87.38
Eupleridae	*Cryptoprocta ferox*	Nocturnal	Closed	Arboreal	54.13	46.40	30.54	103.63
Eupleridae	*Eupleres goudotii*	Crepuscular	Closed	Terrestrial	53.20	42.84	22.12	79.09
Eupleridae	*Fossa fossana*	Nocturnal	Closed	Terrestrial	50.14	46.66	40.53	84.80
Felidae	*Acinonyx jubatus*	Diurnal	Opened	Terrestrial	72.38	41.65	52.77	155.01
Felidae	*Caracal caracal*	Nocturnal	Mixed	Terrestrial	64.27	48.95	48.15	108.82
Felidae	*Homotherium serum*[†]	–	–	–	66.93	37.24	37.36	264.14
Felidae	*Leopardus colocolo*	Diurnal	Opened	Terrestrial	67.27	47.61	47.84	83.86
Felidae	*Leopardus geoffroyi*	Nocturnal	Mixed	Terrestrial	65.75	45.05	41.53	94.19
Felidae	*Leopardus guigna*	Nocturnal	Closed	Terrestrial	67.90	43.11	42.17	79.89
Felidae	*Leopardus pardalis*	Nocturnal	Closed	Terrestrial	66.53	51.38	49.70	120.06
Felidae	*Leopardus wiedii*	Nocturnal	Closed	Arboreal	67.61	49.91	51.60	83.00
Felidae	*Leptailurus serval*	Nocturnal	Opened	Terrestrial	65.80	48.11	50.01	105.69
Felidae	*Lynx canadensis*	Nocturnal	Closed	Terrestrial	66.01	43.93	44.72	103.00
Felidae	*Lynx lynx*	Nocturnal	Closed	Terrestrial	65.67	44.97	48.53	129.72
Felidae	*Lynx pardinus*	Nocturnal	Closed	Terrestrial	70.03	45.10	49.39	111.71
Felidae	*Lynx rufus*	Nocturnal	Mixed	Terrestrial	72.52	43.81	51.64	101.77
Felidae	*Panthera leo*	Nocturnal	Abierta	Terrestrial	53.41	53.25	39.95	278.68
Felidae	*Panthera onca*	Nocturnal	Closed	Terrestrial	57.42	57.28	45.44	207.86
Felidae	*Panthera pardus*	Nocturnal	Mixed	Terrestrial	59.19	55.33	46.96	165.04
Felidae	*Panthera tigris*	Nocturnal	Closed	Terrestrial	58.24	54.97	45.94	288.63
Felidae	*Pardofelis marmorata*	Diurnal	Closed	Terrestrial	69.35	51.69	56.01	79.42
Felidae	*Prionailurus bengalensis*	Nocturnal	Closed	Terrestrial	60.13	53.24	48.12	89.56
Felidae	*Prionailurus viverrinus*	Nocturnal	Mixed	Terrestrial	63.07	50.74	43.43	111.24
Felidae	*Prionailurus rubiginosus*	Nocturnal	Closed	Arboreal	62.20	49.99	45.29	61.20
Felidae	*Puma concolor*	Nocturnal	Mixed	Terrestrial	69.12	47.80	46.61	169.57
Felidae	*Puma yagouarundi*	Diurnal	Mixed	Arboreal	67.99	45.55	42.96	80.46
Felidae	*Smilodon fatalis*[†]	–	–	–	70.33	38.19	41.08	281.28
Herpestidae	*Herpestes edwardsi*	Diurnal	Closed	Terrestrial	67.57	34.77	27.76	64.24
Herpestidae	*Herpestes ichneumon*	Diurnal	Mixed	Terrestrial	68.62	35.36	29.55	69.80
Herpestidae	*Herpestes javanicus*	Diurnal	Closed	Terrestrial	72.73	32.04	30.31	69.80
Herpestidae	*Mungos mungo*	Diurnal	Mixed	Terrestrial	66.29	37.76	26.89	63.50
Herpestidae	*Suricata suricatta*	Diurnal	Opened	Terrestrial	71.15	41.79	44.01	51.57
Hyaenidae	*Crocuta crocuta*	Nocturnal	Mixed	Terrestrial	63.20	38.20	32.92	105.97

(continued)

Table 1 (continued)

Family	Specie	Activity	Habitat	Substrate	α (°)	β (°)	Ω (°)	Sk. Length (mm)
Hyaenidae	*Hyaena hyaena*	Nocturnal	Opened	Terrestrial	59.26	42.96	43.18	249.23
Hyaenidae	*Proteles cristata*	Nocturnal	Opened	Terrestrial	68.58	41.69	42.77	115.53
Mustelidae	*Aonyx capensis*	Diurnal	Closed	Aquatic	55.63	49.08	38.69	113.76
Mustelidae	*Eira barbara*	Diurnal	Closed	Terrestrial	64.97	46.62	41.35	103.14
Mustelidae	*Enhydra lutris*	Diurnal	Opened	Aquatic	57.63	41.75	19.94	123.24
Mustelidae	*Galictis vittata*	Diurnal	Closed	Terrestrial	60.84	43.51	30.44	80.24
Mustelidae	*Ichneuma striatus*	Nocturnal	Mixted	Terrestrial	57.91	46.65	30.24	61.95
Mustelidae	*Ichneumia albicauda*	Nocturnal	Mixted	Terrestrial	68.75	37.14	33.95	87.85
Mustelidae	*Lutra lutra*	Nocturnal	Mixted	Aquatic	48.01	42.13	45.57	218.39
Mustelidae	*Martes americana*	Nocturnal	Closed	Terrestrial	56.31	42.49	24.28	66.55
Mustelidae	*Martes foina*	Nocturnal	Mixted	Terrestrial	60.62	45.27	36.94	74.83
Mustelidae	*Martes pennanti*	Crepuscular	Closed	Terrestrial	55.88	48.50	32.75	101.08
Mustelidae	*Meles meles*	Nocturnal	Mixted	Terrestrial	56.70	46.63	33.05	119.47
Mustelidae	*Mephitis mephitis*	Nocturnal	Mixted	Terrestrial	62.35	39.11	24.57	61.57
Mustelidae	*Mustela nigripes*	Nocturnal	Opened	Terrestrial	49.21	49.18	26.41	63.41
Mustelidae	*Pteronura brasiliensis*	Diurnal	Mixted	Aquatic	38.96	55.40	15.61	142.31
Mustelidae	*Taxidea taxus*	Nocturnal	Mixted	Terrestrial	50.72	51.32	23.59	115.57
Odobenidae	*Odobenus rosmarus*	Diurnal	Opened	Aquatic	65.67	25.86	12.15	332.06
Otariidae	*Arctocephalus australis*	Diurnal	Opened	Aquatic	50.90	43.94	10.65	194.88
Otariidae	*Callorhinus ursinus*	Diurnal	Opened	Aquatic	43.58	57.89	9.13	159.70
Otariidae	*Eumetopias jubatus*	Diurnal	Opened	Aquatic	66.03	30.09	20.25	342.61
Otariidae	*Otaria flavescens*	Diurnal	Opened	Aquatic	61.87	33.29	17.58	269.34
Otariidae	*Zalophus californianus*	Diurnal	Opened	Aquatic	56.12	38.26	11.31	205.09
Phocidae	*Cystophora cristata*	Diurnal	Opened	Aquatic	36.81	61.32	18.28	225.32
Phocidae	*Erignathus barbatus*	Diurnal	Opened	Aquatic	35.75	60.26	14.97	109.43
Phocidae	*Histriophoca fasciata*	Diurnal	Opened	Aquatic	38.08	55.15	9.62	179.86
Phocidae	*Hydrurga leptonyx*	Diurnal	Opened	Aquatic	40.88	52.88	11.45	347.21
Phocidae	*Leptonychotes weddellii*	Diurnal	Opened	Aquatic	36.20	57.04	19.64	281.83
Phocidae	*Lobodon carcinophaga*	Diurnal	Opened	Aquatic	49.62	44.46	6.03	233.94
Phocidae	*Mirounga angustirostris*	Diurnal	Opened	Aquatic	31.44	61.98	11.37	378.88
Phocidae	*Mirounga leonina*	Diurnal	Opened	Aquatic	34.03	61.46	13.77	355.16
Phocidae	*Monachus monachus*	Diurnal	Opened	Aquatic	40.93	58.13	17.73	242.13
Phocidae	*Monachus tropicalis*	Diurnal	Opened	Aquatic	38.00	61.46	20.65	258.85
Phocidae	*Pagophilus groenlandicus*	Diurnal	Opened	Aquatic	33.48	59.65	5.55	197.77
Phocidae	*Phoca vitulina*	Diurnal	Opened	Aquatic	36.25	59.39	8.10	156.24
Phocidae	*Pusa hispida*	Diurnal	Opened	Aquatic	30.01	66.10	9.89	149.38
Procyonidae	*Bassaricyon alleni*	Crepuscular	Closed	Arboreal	65.85	48.31	44.92	71.42
Procyonidae	*Bassaricyon gabbii*	Nocturnal	Closed	Arboreal	68.43	47.94	50.80	73.31
Procyonidae	*Nasua narica*	Diurnal	Closed	Arboreal	64.12	40.24	29.63	61.83
Procionidae	*Nasua nasua*	Diurnal	Closed	Arboreal	54.10	46.80	26.49	101.10
Procyonidae	*Potos flavus*	Nocturnal	Closed	Arboreal	70.87	48.89	46.09	68.99
Procyonidae	*Procyon lotor*	Nocturnal	Mixted	Terrestrial	56.87	55.98	38.76	101.04
Ursidae	*Ailuropoda melanoleuca*	Diurnal	Closed	Terrestrial	53.09	48.76	30.51	128.00
Ursidae	*Helarctos malayanus*	Nocturnal	Closed	Terrestrial	71.59	48.63	52.05	238.64
Ursidae	*Melursus ursinus*	Nocturnal	Mixted	Terrestrial	63.89	48.54	44.48	194.04
Ursidae	*Tremarctos ornatus*	Diurnal	Mixted	Terrestrial	66.26	50.31	49.09	201.90
Ursidae	*Ursus americanus*	Diurnal	Closed	Terrestrial	70.64	42.36	43.31	235.83
Ursidae	*Ursus arctos*	Crepuscular	Mixted	Terrestrial	69.55	48.76	50.75	286.83
Ursidae	*Ursus maritimus*	Diurnal	Opened	Aquatic	68.68	43.94	43.86	335.63
Ursidae	*Ursus thibetanus*	Diurnal	Mixted	Terrestrial	65.44	50.36	44.88	232.76
Viverridae	*Arctictis binturong*	Nocturnal	Closed	Arboreal	61.80	46.52	38.49	138.36
Viverridae	*Cynogale bennettii*	Nocturnal	Closed	Aquatic	58.60	46.61	33.67	109.50
Viverridae	*Paguma larvata*	Nocturnal	Closed	Terrestrial	48.70	57.54	41.49	116.89
Viverridae	*Paradoxurus hermaphroditus*	Nocturnal	Closed	Terrestrial	52.61	59.04	34.98	102.88
Viverridae	*Viverra tangalunga*	Nocturnal	Closed	Terrestrial	52.40	45.92	30.61	112.80

†denote extinct taxa.

plane is defined as the plane that contains the orbitale superius (Os), the orbitale lateralis (Ol) and the most posterior point of the temporal fossa (Tp) (Fig. 1C).

As the carnivores included in our sample lack the postorbital bar, we used the Op instead of the most inferior point of the orbit, the orbitale inferior (Oi, in Heesy, 2008) to define the orbital plane. We used Op because it is a better landmark for defining the plane of the orbit than Oi, as the latter seems more influenced by the shape of the tooth row than is the former in carnivores (C. Casares-Hidalgo, pers. obs.). Moreover, the distance between Oa and Op is longer than between Oa and Oi, better capturing the variation in convergence (Fig. 1C). However, as in the Heesy (2008) dataset several taxa have a postorbital bar, his selection of Oi as a landmark to define the orbit plane was an adequate one.

The orbit orientation was defined by the frontation (α), convergence (β), and orbitotemporal (Ω) angles (e.g. Cartmill, 1970; Heesy, 2008). The frontation angle (α) is measured as the dihedral angle between the dorsal plane and the orbital plane (Fig. 1D). The convergence angle (β) is defined as the dihedral angle between the orbit and sagittal planes (Fig. 1B). The dihedral angle between the orbital and temporal planes (Fig. 1C) is defined here as the orbitotemporal angle (Ω). This angle was taken specifically for this study to characterize the relationship between the orbit and the disposition of the neurocranium and temporal muscles (Cartmill, 1974, 2017; Heesy, 2004, 2005, 2008; Finarelli & Goswami, 2009). We wrote a routine in Wolfram Mathematica v. 11.1 (available from the authors upon request) to calculate the dihedral angles between planes.

The orientation angles were measured on the left and right sides, and they were averaged per specimen to avoid possible undesirable effects due to fluctuating asymmetry. Afterwards, all the specimens per species were averaged to avoid possible effects of static allometry.

Ecological variables

We classified all living species sampled in this study according to (1) their visual strategy (i.e. photopic, scotopic or mesopic); (2) the type of habitat they inhabit (i.e. open, mixed or closed); and (3) their substrate preference (i.e. arboreal, terrestrial or aquatic). We classified photopic carnivores as those species that are active (i.e. hunting or breeding behaviour) in the presence of bright light/photopic conditions, scotopic carnivores as those being active in low-light conditions, and mesopic carnivores as those being active during twilight and/or sunrise (crepuscular) or indifferently during day and night (cathemeral). We classified the type of habitat (open, mixed or closed) according to the value of vegetation cover (Table 1). Carnivores that forage in trees (i.e. hunting or breeding behaviour) have been classified as arboreal. In contrast, those species that forage in aquatic environments (at least partially) and show adaptations for swimming or diving have been classified as aquatic. The rest of the species that usually forage on the ground have been classified as terrestrial.

The information about these ecological variables was taken from the IUCN database (http://www.iucnredlist.org), the PanTHERIA online database (http://esapubs.org/Archive/ecol/E090/184/default.htm) and, when the information was insufficient or doubtful, from Mammalian Species (http://www.science.smith.edu/msi/), Nowak (2005), Sillero-Zubiri et al. (2004), and Wilson & Mittermeier (2009).

Fig. 2 Phylogenetic tree for the species sampled in this paper. The supertree of Nyakatura & Bininda-Emonds (2012) has been pruned to include only the species sampled in our study, and we have included the extinct sabre-tooths using the topology and branch lengths of Piras et al. (2013). Asterisks denote pinnipeds.

orbital, sagittal, and temporal planes (Fig. 1B–D). Their 3D coordinates (*x*, *y*, *z*) were imported into Excel using the Immersion software package (Immersion, Inc., San Jose, CA, USA). We also constructed an additional plane, i.e. the dorsal plane (Fig. 1D), perpendicular to the sagittal plane. The sagittal plane was defined with the points Pr (Prostion), Nn (Nasion), In (Inion), and Bs (Basion; Fig. 1A,B). The orbital plane is defined as the plane that contains the following points: the orbitale superius (Os), the orbitale anterius (Oa) and the orbitale posterius (Op). The temporal

Quantifying the influence of phylogeny

To assess the presence of phylogenetic signal in orbit orientation, we assembled a phylogenetic tree (Fig. 2) using Mesquite (Maddison & Maddison, 2016). We pruned the molecular supertree of Nyakatura & Bininda-Emonds (2012) to exclude those carnivorous species do not sampled in this study. The extinct sabre-tooths were incorporated using the topology and branch length published by Piras et al. (2013).

We calculated the K statistic for continuous traits (Blomberg et al. 2003) for the frontation (α), convergence (β), and orbitotemporal (Ω) angles using the function *phylosig* in the phytools R package (Revell, 2012). The index assumes a Brownian motion (BM) evolutionary model [i.e. purely neutral (random) evolution of a trait with variance directly proportional to the branch lengths] and varies from 0 to $\gg$ 1, where 0 indicates no phylogenetic signal (the trait has evolved independently of phylogeny, and close relatives are not more similar than distant relatives) and values > 1 reflect that close relatives are more similar than expected under BM. Interestingly, the K statistic has the advantage of allowing direct comparison of phylogenetic signal strengths not only across traits but also across different phylogenetic trees (Molina-Venegas & Rodríguez, 2017). The statistical significance of K was assessed based on a comparison of the observed phylogenetically independent contrasts and the expected contrast under 999 randomizations (Blomberg et al. 2003).

Additionally, we calculated Pagel's λ (Pagel, 1993) to assess the degree of phylogenetic signal in the frontation, convergence, and orbitotemporal angles using the function *phylosig* in the phytools R package (Revell, 2012). Pagel's λ is a parameter for the correlations between species relative to the correlation expected under Brownian evolution. It scales between zero (indicating an absence of correlation between species) and 1.0 (indicating a correlation between species equal to the Brownian expectation).
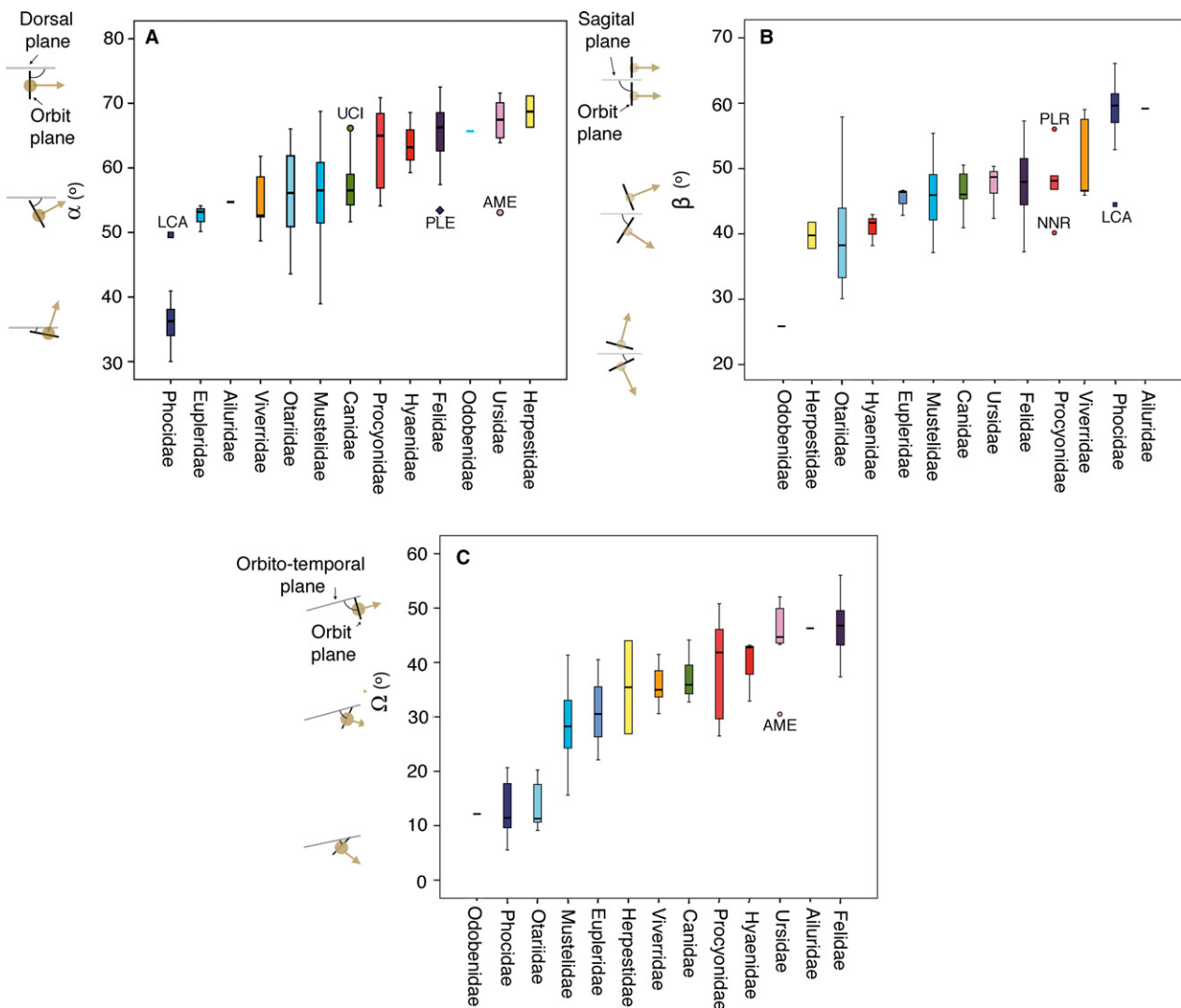

Fig. 3 Box plots showing the range of frontation (α), convergence (β), and orbitotemporal (Ω) angles across all carnivoran families analysed here. The vertical line inside each box is the median. Box length is the interquartile range (IQR) and shows the difference between the 75th and 25th percentiles. Horizontal bars enclose values of 5–95%. UCI, *Urocyon cinereoargenteus*; PLE, *Panthera leo*; AME, *Ailuropoda melanoleuca*; PLR, *Procyon lotor*; NNR, *Nasua narica*; LCA, *Lobodon carcinophaga*.

To reconstruct the past phenotypes of extinct ancestral species from the trait values of their extant descendants, we mapped the frontation, convergence, and orbitotemporal angles on the phylogeny of Fig. 2. Using the R package phytools (Revell, 2012), we estimated the ancestral characters at internal nodes assuming a Brownian mode of evolution. However, it is worth mentioning that these analyses should be used with caution, as potential inaccuracy in reconstructing ancestral traits of the internal nodes of the phylogeny in the absence of fossil taxa has been demonstrated (Finarelli & Flynn, 2006).

The influence of skull length on orbit orientation and the relationships between orbit angles

We explored the relationship between orbit orientation and body size to control for allometric effects, as Changizi & Shimojo (2008) demonstrated that orbit convergence increases with body size for species in forests but not in other leafy and semi-leafy environments. Therefore, as body size could be a determinant of orbit orientation, we decided to test for allometry in orbit angles as a preliminary test to discard possible allometric effects on the orbit of mammalian carnivores. Accordingly, we regressed α, β, and Ω with skull length as a proxy for carnivore body size (Van Valkenburgh, 1990). This was tested with ordinary least squares (OLS) regression analysis of log-transformed variables. We also explored the relationships among the angles (α–β, α–Ω, and β–Ω) using OLS regression analysis of log-transformed variables with PAST (Hammer & Harper, 2004).

However, species cannot be treated as statistically independent data points because they are phylogenetically related (Felsenstein, 1985). This violates the assumption of independent sampling and hence inflates the classic type I error (e.g. Harvey & Pagel, 1991). To avoid this, we performed phylogenetic generalized least square (PGLS) analysis (Martins & Hansen, 1997) using the geiger package of R (Harmon et al. 2007) with 10 000 permutations and using a Brownian motion model of evolution.

Testing the influence of ecology on orbit orientation

To assess the relationship of orbit orientation with the ecological variables, we used phylogenetic MANOVA (Garland et al. 1993) with α,

Table 2 Summary statistics for bivariate regressions computed to test the influence of skull length on orbit orientation as well as the relationships between the angles.

Regressions	Model	r^2	F	P-value
α-Skl	OLS	0.0829	0.0500	< 0.01
	PGLS	0.0021	0.2187	0.691
β-Skl	OLS	0.0005	0.0500	> 0.05
	PGLS	0.0089	0.9331	0.405
Ω-Skl	OLS	0.1253	14.8660	< 0.01
	PGLS	0.0065	0.6800	0.490
α-β	OLS	0.4020	69.8950	< 0.01
	PGLS	0.4507	85.3290	< 0.01
α-Ω	OLS	0.5715	139.1380	< 0.01
	PGLS	0.0788	8.8904	0.008
β-Ω	OLS	0.0202	2.1530	> 0.05
	PGLS	0.0042	0.4358	0.589

β, and Ω as a multivariate response variable and visual strategy, substrate preference, and type of habitat as predictor variables, all while taking phylogeny into account. We used the aov.phylo function in the geiger package of R (Harmon et al. 2007), assuming Brownian motion. For obvious reasons, both of the sabre-tooths were excluded from the analysis. We used a Brownian model of evolution and 1000 replicates to test for statistical significance. To test for specific relationships among pairs of predictor and response variables while taking phylogeny into account, we also used phylogenetic ANOVA (Garland et al. 1993).

Depicting the orbit orientation phylomorphospace

To investigate the distribution of carnivorans in phenotypic space, we computed a principal components analysis (PCA) from the correlation matrix of the log-transformed frontation, convergence, and orbitotemporal angles and skull length in the 104 species analysed. Another PCA was performed excluding pinnipeds from the same log-transformed variables.

The reconstructed ancestral values were plotted into the shape spaces obtained in the PCAs. Subsequently, the branches of the tree were connected (Klingenberg & Ekau, 1996; Rohlf, 2002; Polly, 2008; Astúa, 2009; Gidaszewski et al. 2009; Figueirido et al. 2010, 2013, 2016; Klingenberg & Gidaszewski, 2010) to construct orbit phylomorphospaces. We used the function phylomorphospace in the phytools R package (Revell, 2012).

Results and Discussion

Inter-family differences in orbit orientation

The values of frontation (α), convergence (β), and orbitotemporal (Ω) angles across all the carnivoran families are shown as box plots in Fig. 3. The families in these boxplots are ordered according to the increasing value in each orbit angle.

The family Phocidae shows the lowest values of frontation among the sample (Fig. 3A), which a priori could be interpreted as an adaptation to have the orbits facing upwards as a consequence of diving in the mesopelagic zone (e.g. Levenson & Schusterman, 1999). However, otariids have similar values of frontation to other fissipeds, but contrary to phocids, they are adapted to forage in the epipelagic zone. Moreover, the giant otter (*Pteronura brasiliensis*), which is the mustelid with the lowest frontation angle in our sample and overlapping with the values of phocids, does not dive in deep zones (Carter & Rosas, 1997), and the deepest-diving marine otter (*Enhydra lutris*) has a value of frontation similar to other mustelids. The walrus (*Odobenus rosmarus*) has the lowest value of convergence (Fig. 3B).

Strikingly, pinnipeds have the lowest values of orbitotemporal angles and are well differentiated from fissipeds (Fig. 3C). Among fissipeds, the families with the largest orbitotemporal angles are felids, the red panda and ursids (Fig. 3C), and those with low orbitotemporal angles are mustelids and euplerids (Fig. 3C).
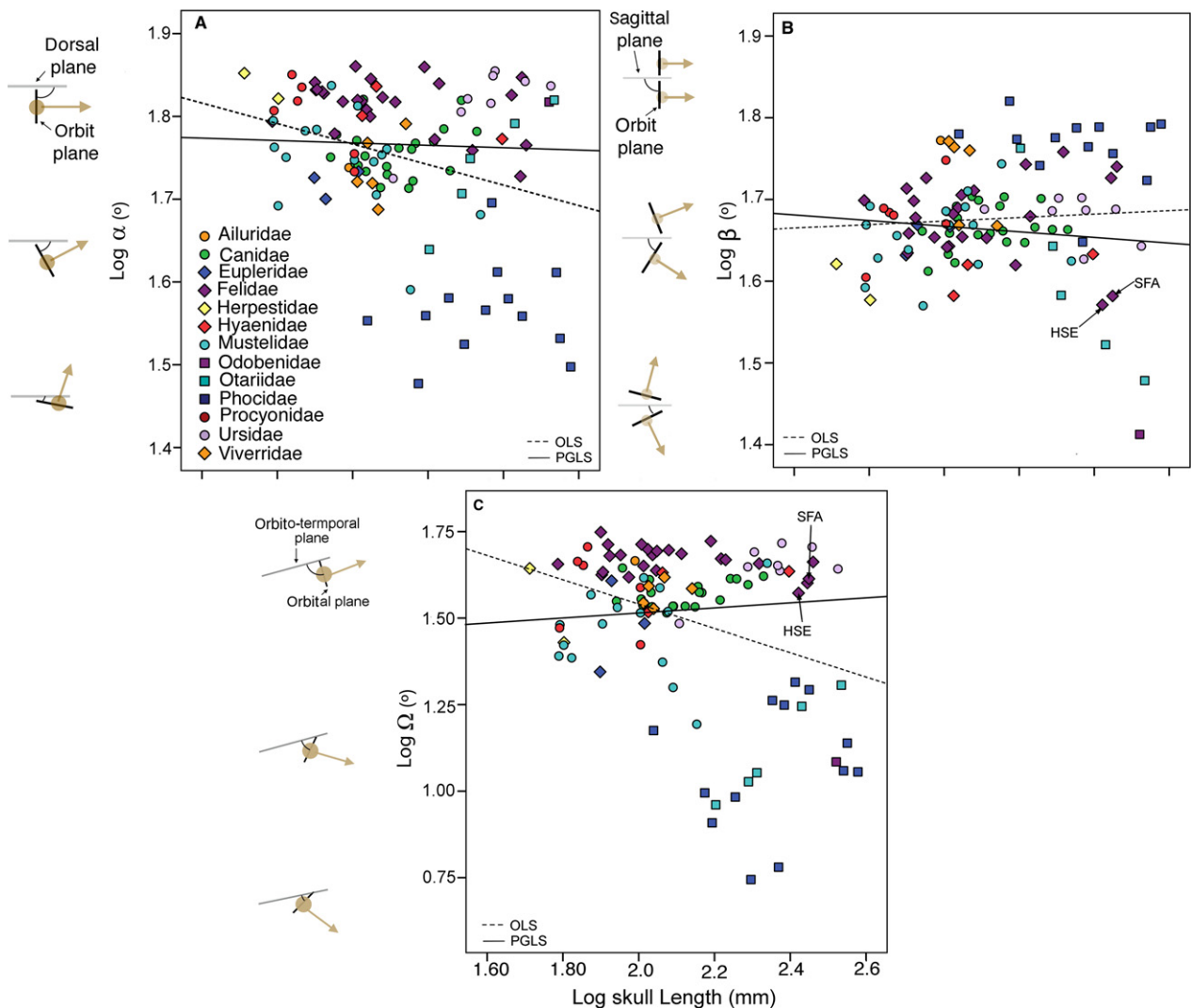
Fig. 4 Bivariate plots of orbit angles against skull length. (A) Skull length against frontation angle (α). (B) Skull length against convergence angle (β). (C) Skull length against orbitotemporal angle (Ω).All variables are log-transformed. HSE, *Homotherium serum*; SFA, *Smilodon fatalis*. Dotted line, regression line using ordinary least squares (OLS); Black line, regression line using phylogenetic generalized least squares (PGLS). All variables are log-transformed.

Skull length does not influence orbit orientation

The linear regression analysis of frontation and orbitotemporal angles against skull length indicated that both angles are associated with size (Table 2; Fig. 4A,C). However, both significant associations disappeared when taking the phylogenetic relationships of species into account (Table 2; Fig. 4A,C). In contrast, the linear regression analysis of orbit convergence against skull length was not significant (Table 2; Fig. 5B).

Therefore, our data suggest that orbit orientation in carnivores is not influenced by skull length, which means that longer or shorter skulls are not characterized by specific orbit orientations. However, although we included a sample with a wide range of body masses, according to Cartmill

(2017) orbit orientation is not ever expected to vary with size across large size ranges.

The relationships between angles

The linear regression analysis of frontation against convergence was highly significant, even when the phylogenetic relationships were taken into account (Table 2; Fig. 5A). It is striking that, at least in mammalian carnivores, an increase in frontation entails a decrease in convergence and vice versa, which indicates that not all combinations of frontation/convergence are possible.

Similarly, the linear regression analysis of frontation compared with the orbitotemporal angle was highly significant,
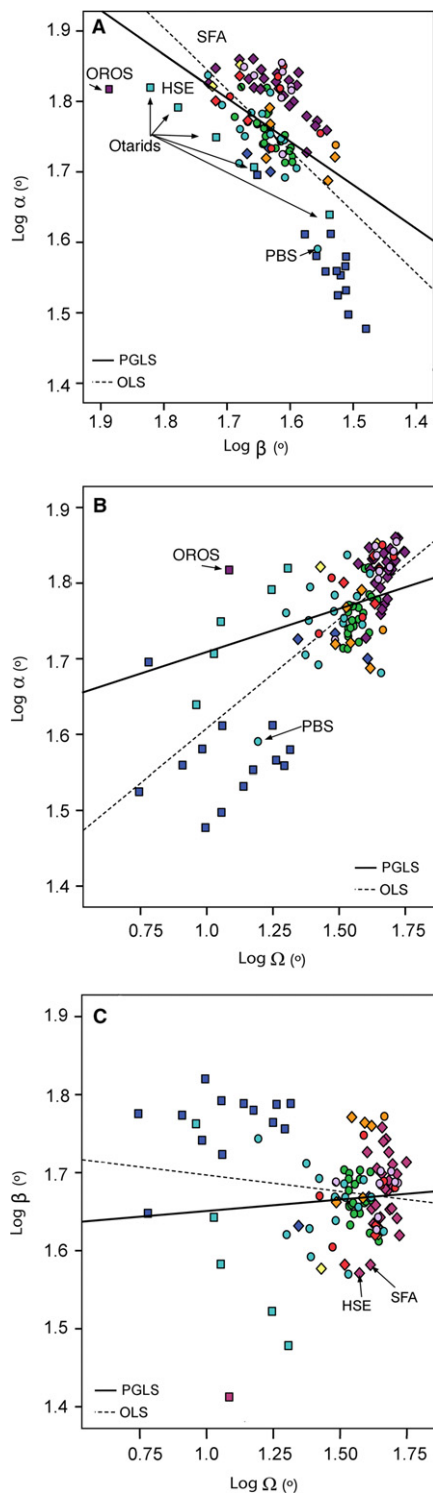
Fig. 5 Bivariate plots of the association among orbit angles. (A) Frontation (α) against convergence (β). (B) Orbitotemporal (Ω) against convergence (β). (C) Convergence (β) against orbitotemporal (Ω). All variables are log-transformed. Black line, regression line using ordinary least squares (OLS); dotted line, regression line using phylogenetic generalized least squares (PGLS). HSE, *Homotherium serum*; SFA, *Smilodon fatalis*; PBS, *Pteronura brasiliensis*; OROS, *Odobenus rosmarus*.

even when phylogeny was taken into account (Table 2; Fig. 5B). On the other hand, the linear regression analysis between convergence and the orbitotemporal angle was not significant (Table 2; Fig. 5C).

A strong influence of phylogeny on orbit orientation

Orbit orientation in carnivores exhibited a significant phylogenetic signal, as indicated by both Bloomberg's K and Pagel's lambda (α: $K = 0.7308$, P-value $= 0.001$; $\lambda = 0.994$, P-value < 0.001; β: $K = 0.338$; P-value < 0.001; $\lambda = 0.984$; P-value < 0.001; Ω: $K = 0.806$; P-value < 0.001; $\lambda = 0.872$).

Mapping the values of orbit angles on the phylogenetic tree of Fig. 2, it is possible to trace the history of these traits through the evolution of the clade. Strikingly, different groups have acquired larger frontation values than the one reconstructed for the common ancestor of all carnivoran families (e.g. ursids, canids, procyonids). This indicates that larger frontation angles seem to have evolved independently in multiple groups of carnivorans (α; Fig. 6A). In contrast, the evolution of convergence (β; Fig. 6B) seem to be more conservative, although multiple groups also experience the independent acquisition of larger convergence values (e.g. pantherines or phocids) and few cases experience a decrease in convergence values (i.e. *Odobenus rosmarus* and *Eumetopias jubatus*). It is also important to note that the distribution of values of the orbitotemporal angle is similar to frontation (Ω; Fig. 5C).

Orbit orientation is not related to ecology

Non-phylogenetic MANOVA revealed that orbit orientation was statistically associated with visual strategy, habitat, and substrate preference (Table 3). Taking the phylogenetic relationships of the species into account, orbit orientation was statistically associated with neither visual strategy nor habitat use (Table 3). However, the significant association of orbit orientation with substrate preference (Table 3) was probably due to the ecological homogeneity among pinnipeds. Pinnipeds [Phocidae (earless or true seals), Otariidae (sea lions and fur seals), and Odobenidae (one extant species of walrus)] have particularly long skulls and a unique combination of frontation, convergence, and orbitotemporal angles. Moreover, they are aquatic, diurnal, and inhabit the same areas. As a matter of fact, when we repeated the analyses excluding pinnipeds, the association between orbit orientation and substrate preference was not significant (Table 3).

To detect which predictor (independent) variable specifically influences a given response (dependent) variable, we performed a set of phylogenetic ANOVA to test for specific associations between pairs of variables. Accordingly, frontation was directly associated with habitat and substrate preference, even when taking the phylogenetic relationships of the species into account (Table 4). On the other hand, the
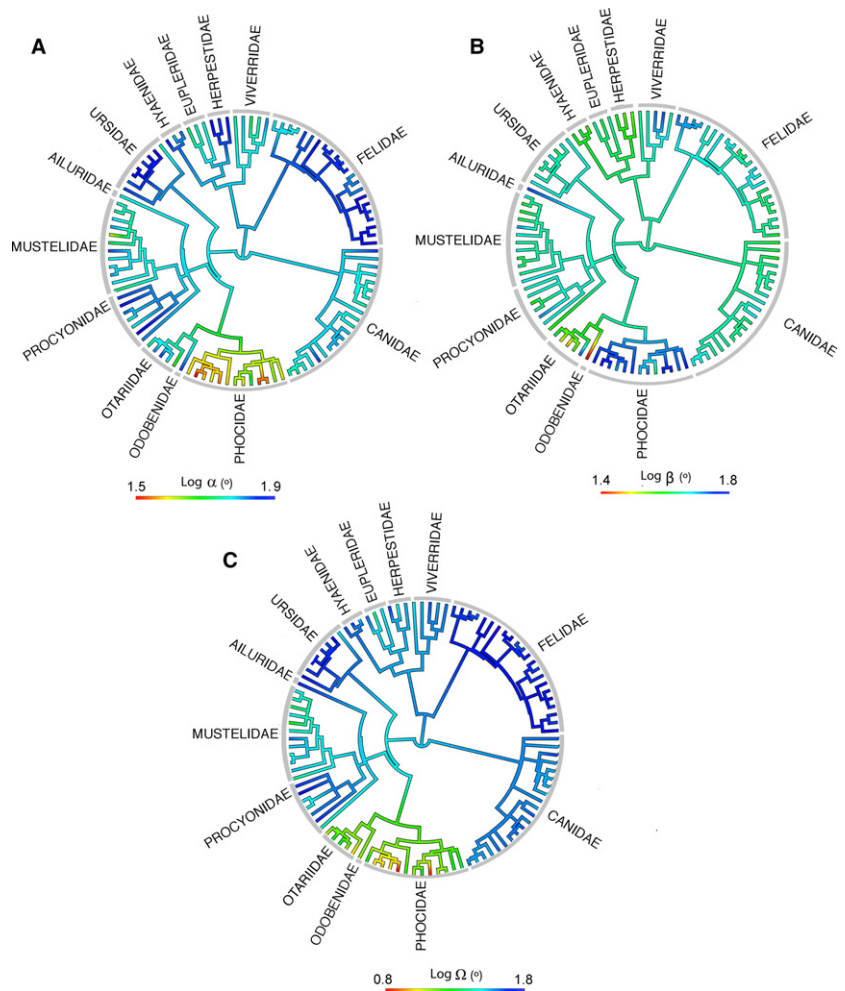
Fig. 6 Values of (A) frontation (α), (B) convergence (β), and (C) orbitotemporal angles (Ω) plotted on the phylogenetic tree for the species sampled in this paper.

Table 3 Results obtained from phylogenetic MANOVA using Brownian model of evolution and 1000 simulations.

	df	Wilks' lambda	Approx-F	num-df	den-df	P	Pphy
Sample including pinnipeds							
Activity	2	0.643	8.142	6	198	0.000	0.120
Habitat	2	0.684	6.907	6	198	0.000	0.054
Substrate	2	0.331	24.332	6	198	0.000	0.005
Sample excluding pinnipeds							
Activity	2	0.836	2.504	6	160	0.024	0.289
Habitat	2	0.750	4.122	6	160	0.001	0.071
Substrate	2	0.829	2.628	6	160	0.019	0.112

P, standard (non-phylogenetic) P-value; Pphy, phylogenetic P-values; df, degrees of freedom.

orbitotemporal angle was statistically associated with habitat vision and substrate preference, even when taking phylogeny into account (Table 4). However, all these significant associations disappeared when we re-analysed the data

excluding pinnipeds, with the exception of the association between the orbitotemporal angle and substrate preference (Table 4). However, we urge readers to interpret these results with caution, as this significant association may simply be a statistical artefact, given that randomization could inflate the degrees of freedom, and hence giving a 'false-positive' result in statistical tests. In any case, as the orbitotemporal angle reflects to a great extent the disposition of masticatory muscles – mainly the temporalis and masseter muscles (Cartmill, 1970; Heesy, 2005), the observed association between the orbitotemporal angle and the use of substrate could be indirectly reflecting a feeding diet requiring special cranial adaptations (e.g. Figueirido et al. 2010).

Orbit orientation phylomorphospace

The phylomorphospace depicted from the superimposition of the phylogeny shown in Fig. 2 onto the bivariate plot, depicted from the first two PCs obtained from PCA of orbit orientation, is shown in Fig. 7. Figure 7A depicts the phylomorphospace from the sample of fissipeds plus pinnipeds.

Table 4 Results obtained from phylogenetic ANOVA using Brownian model of evolution and 1000 simulations.

		df	Sum-Sq	Mean-Sq	*F*-value	*P*	*P*phy
Sample including pinnipeds							
Alpha	Vision	2.000	0.109	0.055	8.053	0.001	0.252
	Habitat	2.000	0.163	0.082	13.034	0.000	0.032
	Substrate	2.000	0.328	0.164	35.435	0.000	0.028
Beta	Vision	2.000	0.002	0.001	0.220	0.803	0.957
	Habitat	2.000	0.004	0.002	0.458	0.634	0.843
	Substrate	2.000	0.011	0.005	1.301	0.277	0.829
Omega	Vision	2.000	1.760	0.880	25.446	0.000	0.009
	Habitat	2.000	1.413	0.706	18.584	0.000	0.012
	Substrate	2.000	3.437	1.719	95.640	0.000	0.001
Sample excluding pinnipeds							
Alpha	Vision	2.000	0.004	0.002	0.747	0.477	0.795
	Habitat	2.000	0.002	0.001	0.354	0.703	0.824
	Substrate	2.000	0.013	0.007	2.647	0.077	0.361
Beta	Vision	2.000	0.003	0.002	0.927	0.400	0.743
	Habitat	2.000	0.007	0.003	1.879	0.159	0.348
	Substrate	2.000	0.003	0.001	0.723	0.488	0.760
Omega	Vision	2.000	0.023	0.012	1.040	0.358	0.713
	Habitat	2.000	0.009	0.004	0.376	0.688	0.792
	Substrate	2.000	0.163	0.081	8.516	0.000	0.032

P, standard (non-phylogenetic) test; *P*phy, phylogenetic *P*-values; df, degrees of freedom.

Whereas PCI explains 55.45% of the original variance, PCII explain 25.30%, which jointly explains more than 80% of the original variance. The scores of the species on this phylomorphospace reveal a clear separation between fissipeds and pinnipeds. Species with high scores on PCI have very high values of frontation and orbitotemporal angles, and very low values of skull length and convergence. Species with low scores on PCI are characterized by having high values of convergence and skull length. On the other hand, species with high scores on PCII are characterized by very high convergence values and moderate orbitotemporal ones. Those species scoring negatively on this eigenvector are characterized by high values of skull length and frontation angle.

The combination of both PCs separates pinnipeds from fissipeds in this morphospace (Fig. 7A). While phocids are separated from fissipeds plus otariids and odobenids on PCI, otariids and odobendis are separated from the rest of the sample on PCII. Strikingly, despite the variety of ecologies exhibited by fissipeds in comparison with pinnipeds, they occupy a much lower portion of this morphospace than pinnipeds.

We also performed a second phylomorphospace from PCA computed with a sample restricted to fissipeds (Fig. 7B). The first PC explains 43.10% of the original variance, and the second PC explains 32.36%, which jointly explain more than 75% of the total variation. Whereas on the first PC all variables score positively, excepting the convergence angle, on PCII all variables score positively, excepting frontation. Therefore, ursids, felids, and hyaenids score on the positive end of PCI and the rest of the sample score negatively.

Conclusions

Our results indicate that variation in orbit orientation is not influenced by variation in skull length and therefore allometry has a negligible effect on orbit orientation in mammalian carnivores (Fig. 5; Table 2). The significance of this relationship found in some studies (e.g. Changizi & Shimojo, 2008) could be due to the taxa included in the sample. This does not contradict the 'X-ray hypothesis', but it encourages testing their asseverations from another point of view, such as using a visual axis instead of an orbit axis.

The frontation and convergence angles are negatively correlated, indicating that carnivores with more forward-facing orbits (more convergence) also have more upward-facing orbits (less frontation). In contrast, the frontation and orbitotemporal angles are positively correlated, indicating that carnivores with more downward-facing orbits (more frontation) also have less parallel temporal and orbit planes. This significant association indicates a strong influence of the shape and size of the temporal fossa in shaping frontation. Although further exploration is necessary to infer how modularity and integration in the carnivoran skull can affect orbit orientation, Finarelli & Goswami (2009) demonstrated that encephalization is related to orbit orientation, at least in felids and canids.

Our results also demonstrate that orbit orientation is only statistically associated with substrate preference and not
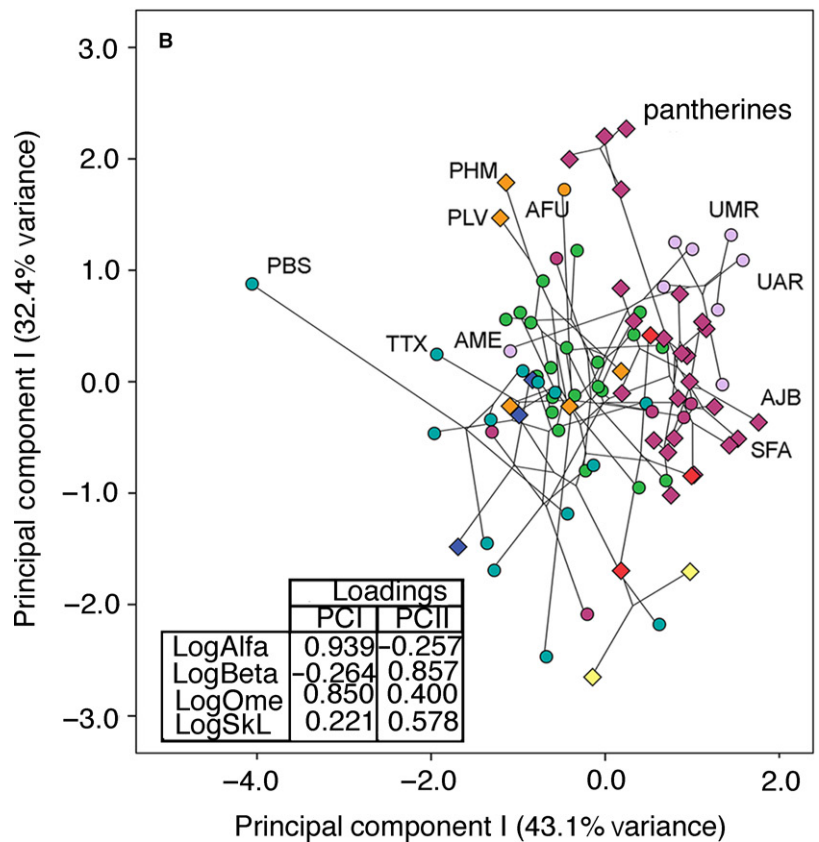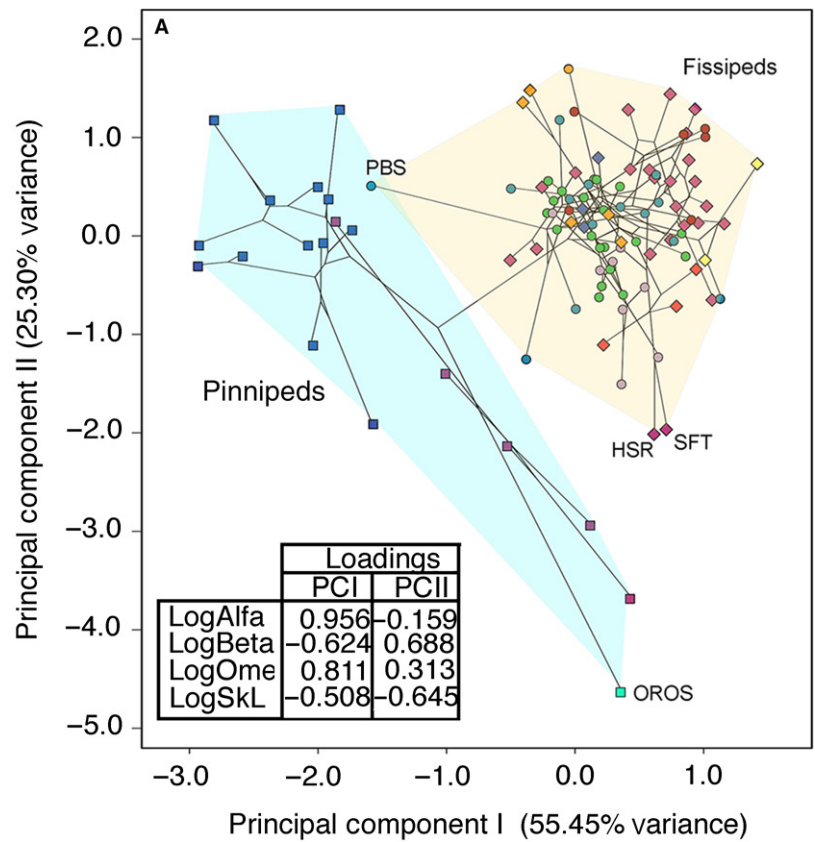
Fig. 7 Phylomorphospaces of orbit orientation and skull length in carnivores. (A) Phylomorphospace depicted from the first two PCs obtained from the PCA computed from the sample of pinnipeds plus fissipeds. (B) Phylomorphospace depicted from the first two PCs obtained from the PCA computed from the sample excluding pinnipeds. AME, *Ailuropoda melanoleuca*; AFU, *Ailurus fulgens*; HSR, *Homotherium serum*; SFT, *Smilodon fatalis*; PBS, *Pteronura brasiliensis*; OROS, *Odobenus rosmarus;* TTX, *Taxidea taxus*; PLV, *Paguma larvata*; PHM, *Paradoxurus hermaphroditus*; UMR, *Ursus maritimus*; UAR, *Ursus arctos*; AJB, *Acinonyx jubatus*. Symbols as in Fig. 4.

with preferred habitat or visual strategy, even when taking phylogeny into account (Table 3). However, when we re-analysed the sample excluding pinnipeds, the association between orbit orientation and substrate preference was not significant (Table 3). Similarly, the analyses performed between specific pairs of orbit angles and ecological variables also revealed significant associations between frontation and the orbitotemporal angles when the complete sample of species was analysed (Table 4). Again, when we re-analysed the data excluding pinnipeds, none of the associations was significant, the sole exception being that between orbitotemporal angle and substrate preference. The reason for the absence of significant correlation between orbit orientation and the ecology of the taxa when pinnipeds are excluded is that they have particularly long skulls and a unique combination of frontation, convergence, and orbitotemporal angles. Moreover, they are all aquatic, diurnal, and inhabit very open areas. Therefore, their presence in the analysis significantly biases the results towards having significant associations.

The significant correlation found between the orbitotemporal angle and substrate preference is probably related to feeding behavior, as the orbitotemporal angle mainly reflects the disposition of masseter and temporalis muscles involved in chewing, gape angle, and struggling with prey (e.g. Figueirido et al. 2010, 2012, 2013) in the case of predators (e.g. pantherines).

In any case, the lack of association between orbit orientation and the visual strategy or the type of habitat of carnivores was totally unexpected. Previous studies have found significant associations between them (e.g. Walls, 1942; Hughes, 1977; Noble et al. 2000; Heesy, 2008), but including more mammalian orders, such as primates, rodents or ungulates. For example, Heesy (2008) showed in a large sample of non-primate eutherian mammals that approximately 40% of the variance in orbit orientation was highly influenced by ecological factors such as activity pattern, substrate preference, and the degree of faunivory.

One explanation for the lack of association between orbit anatomy and visual strategy in carnivores found in our study could be the nocturnal bottleneck hypothesis (see Heesy & Hall, 2010 for a review). The ancestral condition of nocturnality in mammals provided useful adaptations in the eye tissues for the entire range of vision. In fact, several researchers have found evidence for genetic and physiological adaptations related to the nocturnal bottleneck that have not been reflected in the orbit anatomy (e.g. Hut et al. 2000; Hall et al. 2012; Gerkema et al. 2013).

The lack of a significant association between the evolutionary increases or decreases in orbit angles (Fig. 6) among different carnivoran families and the habitat preference could be explained because the ancestral stem carnivoramorphans (early miacoids) acquired a range of orbit angles that were useful for the entire range of ecologies exhibited by derived monophyletic groups of the crown-clade Carnivora. Therefore, the adaptation of different orbit orientations to specific ecological niches has simply been unnecessary. In fact, early Tertiary families of carnivoramorphans, the paraphyletic 'Miacidae' and monophyletic Viverravidae (Wesley-Hunt & Flynn, 2005), which are traditionally joined as Miacoidea (Flynn & Galiano, 1982; Hunt & Tedford, 1993), were ecologically diverse, with species adapted to arboreal, scansorial, and cursorial locomotion, and ranging in size from weasel-sized to coyote-sized forms (Flynn et al. 1998).

If this hypothesis holds, then the orbit anatomy of mammalian carnivorans represents a case of an 'ecological bottleneck' probably acquired in early Cenozoic representatives of stem taxa. However, differences between orbit axis and eye axis (the direction in which the orbits are directed and the direction in which the eyes are watching, respectively) could also explain the lack of correlation in fissipeds between orbit orientation and habitat preference. Cartmill (2017) observed that neither visual nor orbit orientation could be directly inferred from the orientation of the orbits in smaller mammals. In fact, most mammals have conjugate eye movements, i.e. both eyes gaze in the same direction with visual axes directed at the same point in space (Walls, 1942). In other words, orbit orientation does not necessarily reflect visual orientation (Simons, 2009).

In summary, this study demonstrates a lack of association between orbit anatomy and ecology in carnivoran mammals and shows that extrapolating visual strategies and the type of habitat for extinct carnivores from orbit anatomy should be done with caution. Our results also highlight the need to develop more accurate methods to characterize eye axis instead of orbit axis.

Acknowledgements

Conflict of interest

None of the authors has any conflict of interest to declare.

Author contributions

A.P.R., C.C.H. collected the data. C.C.H., B.F. performed the analyses. B.F., C.C.H., F.J.P. designed the study. M.F.G. wrote

the script in MATHEMATICA to calculate the angles. B.F., C.C.H., M.F.G. wrote the paper.

References

Allman J (1977) Evolution of the visual system in the early primates. *Prog Psychobiol Physiol Psychol* 7, 53.

Angielczyk KD, Schmitz L (2014) Nocturnality in synapsids predates the origin of mammals by over 100 million years. *Proc R Soc B* 281, 20141642.

Astúa D (2009) Evolution of scapula size and shape in didelphid marsupials (Didelphimorphia: Didelphidae). *Evolution* 63, 2438–2456.

Blomberg SP, Garland T Jr, Ives AR, et al. (2003) Testing for phylogenetic signal in comparative data: behavioral traits are more labile. *Evolution* 57, 717–745.

Campbell FW, Green DG (1965) Optical and retinal factors affecting visual resolution. *J Physiol* 181, 576–593.

Carter SK, Rosas FC (1997) Biology and conservation of the giant otter *Pteronura brasiliensis*. *Mamm Rev* 27, 1–26.

Cartmill M (1970) *The orbits of arboreal mammals: a reassessment of the arboreal theory of primate evolution*. Doctoral Dissertation, University of Chicago, Department of Anthropology.

Cartmill M (1974) Rethinking primate origins. *Science* 184, 436–443.

Cartmill M (1992) New views on primate origins. *Evol Anthropol Issues News Rev* 1, 105–111.

Cartmill M (2017) Arboreal adaptations and the origin of the order Primates. In: *The Functional and Evolutionary Biology of Primates* (ed. Tuttle R), pp. 97–122. New York: Routledge.

Changizi MA, Shimojo S (2008) "X-ray vision" and the evolution of forward-facing eyes. *J Theor Biol* 254, 756–767.

Crompton RH (1995) Visual predation, habitat structure, and the ancestral primate niche. In: *Creatures of the Dark*. The Nocturnal Prosimians. (eds Alterman L, Doyle GA, Kay Izard M), pp. 11–30. Boston, MA: Springer.

Felsenstein J (1985) Phylogenies and the comparative method. *Am Nat* 125, 1–15.

Figueirido B, Serrano-Alarcón FJ, Slater GJ, et al. (2010) Shape at the cross-roads: homoplasy and history in the evolution of the carnivoran skull towards herbivory. *J Evol Biol* 23, 2579–2594.

Figueirido B, Serrano-Alarcón FJ, Palmqvist P (2012) Geometric morphometrics shows differences and similarities in skull shape between the red and giant pandas. *Journal of Zoology* 286, 293–302.

Figueirido B, Tseng ZJ, Martín-Serra A (2013) Skull shape evolution in durophagous carnivorans. *Evolution* 67, 1975–1993.

Figueirido B, Martín-Serra A, Janis CM (2016) Ecomorphological determinations in the absence of living analogues: the predatory behavior of the marsupial lion (*Thylacoleo carnifex*) as revealed by elbow joint morphology. *Paleobiology* 42, 508–531.

Figueirido B, Lautenschlager S, Pérez-Ramos A, et al. (2018) Distinct predatory behaviors in Scimitar- and Dirk-toothed sabertooth cats. *Curr Biol* 28, 3260–3266.

Finarelli JA, Flynn JJ (2006) Ancestral state reconstruction of body size in the Caniformia (Carnivora, Mammalia): the effects of incorporating data from the fossil record. *Syst Biol* 55, 301–313.

Finarelli JA, Goswami A (2009) The evolution of orbit orientation and encephalization in the Carnivora (Mammalia). *J Anat* 214, 671–678.

Flynn JJ, Galiano H (1982) Phylogeny of early Tertiary Carnivora: with a description of a new species of Protictis from the Middle Eocene of northwestern Wyoming. *Am Mus Novit* no. 2725.

Flynn JJ, Janis CM, Scott KM, et al. (1998) Early Cenozoic Carnivora ('Miacoidea'). *Evol Tertiary Mamm North America* 1, 110–123.

Garamszegi LZ, Møller AP, Erritzøe J (2002) Coevolving avian eye size and brain size in relation to prey capture and nocturnality. *Proc R Soc Lond B Biol Sci* 269, 961–967.

Garland T Jr, Dickerman AW, Janis CM, et al. (1993) Phylogenetic analysis of covariance by computer simulation. *Syst Biol* 42, 265–292.

Gerkema MP, Davies WI, Foster RG, et al. (2013) The nocturnal bottleneck and the evolution of activity patterns in mammals. *Proc R Soc Lond B Biol Sci* 280, 20130508.

Gidaszewski NA, Baylac M, Klingenberg CP (2009) Evolution of sexual dimorphism of wing shape in the *Drosophila melanogaster* subgroup. *BMC Evol Biol* 9, 110.

Hall MI, Kamilar JM, Kirk EC (2012) Eye shape and the nocturnal bottleneck of mammals. *Proc R Soc Lond B Biol Sci* 279, 4962–4968.

Hammer O, Harper DAT (2004) PAST version 1.3. Available from https://folk.uio.no/ohammer/past/

Harmon LJ, Weir JT, Brock CD, et al. (2007) GEIGER: investigating evolutionary radiations. *Bioinformatics* 24, 129–131.

Harvey PH, Pagel MD (1991) *The Comparative Method in Evolutionary Biology*, Vol. 239. Oxford: Oxford University Press.

Heesy CP (2004) On the relationship between orbit orientation and binocular visual field overlap in mammals. *Anat Rec* 281, 1104–1110.

Heesy CP (2005) Function of the mammalian postorbital bar. *J Morphol* 264, 363–380.

Heesy CP (2008) Ecomorphology of orbit orientation and the adaptive significance of binocular vision in primates and other mammals. *Brain Behav Evol* 71, 54–67.

Heesy CP, Hall MI (2010) The nocturnal bottleneck and the evolution of mammalian vision. *Brain Behav Evol* 75, 195–203.

Hughes A (1977) The topography of vision in mammals of contrasting life style: comparative optics and retinal organisation. In: *The Visual System in Vertebrates*. (ed Crescitelli F), pp. 613–756. Berlin: Springer-Verlag.

Hunt RM Jr, Tedford RH (1993) Phylogenetic relationships within the aeluroid Carnivora and implications of their temporal and geographic distribution. In: *Mammal Phylogeny* (eds Novacek MJ, McKenna M, Szalay FS), pp. 53–73. New York: Springer Verlag.

Hut RA, Scheper A, Daan S (2000) Can the circadian system of a diurnal and a nocturnal rodent entrain to ultraviolet light? *J Comp Physiol A* 186, 707–715.

Klingenberg CP, Ekau W (1996) A combined morphometric and phylogenetic analysis of an ecomorphological trend: pelagization in Antarctic fishes (Perciformes: Nototheniidae). *Biol J Linn Soc* 59, 143–177.

Klingenberg CP, Gidaszewski NA (2010) Testing and quantifying phylogenetic signals and homoplasy in morphometric data. *Syst Biol* 59, 245–261.

Levenson DH, Schusterman RJ (1999) Dark adaptation and visual sensitivity in shallow and deep-diving pinnipeds. *Mar Mamm Sci* 15, 1303–1313.

MacIver MA, Schmitz L, Ugurcan M, et al. (2017) Massive increase in visual range preceded the origin of terrestrial vertebrates. *Proc Natl Acad Sci* U S A 114, E2375–E2384.

Maddison WP, Maddison DR (2016) Mesquite: a modular system for evolutionary analysis. Vers. 3.10.

Martins EP, Hansen TF (1997) Phylogenies and the comparative method: a general approach to incorporating phylogenetic information into the analysis of interspecific data. *Am Nat* **149**, 646–667.

Molina-Venegas R, Rodríguez MÁ (2017) Revisiting phylogenetic signal; strong or negligible impacts of polytomies and branch length information? *BMC Evol Biol* **17**, 53.

Motani R, Rothschild BM, Wahl JR (1999) Large eyeballs in diving ichthyosaurs. *Nature* **402**, 747.

Noble VE, Kowalski EM, Ravosa MJ (2000) Orbit orientation and the function of the mammalian postorbital bar. *J Zool* **250**, 405–418.

Nowak RM (2005) *Walker's Carnivores of the World*. Baltimore: JHU Press.

Nyakatura K, Bininda-Emonds OR (2012) Updating the evolutionary history of Carnivora (Mammalia): a new species-level supertree complete with divergence time estimates. *BMC Biol* **10**, 12.

Pagel M (1993) Seeking the evolutionary regression coefficient: an analysis of what comparative methods measure. *J Theor Biol* **164**, 191–205.

Piras P, Maiorino L, Teresi L, et al. (2013) Bite of the cats: relationships between functional integration and mechanical performance as revealed by mandible geometry. *Syst Biol* **62**, 878–900.

Pirenne MH (1943) Binocular and uniocular threshold of vision. *Nature* **152**, 698–699.

Polly PD (2008) Adaptive zones and the pinniped ankle: a 3D quantitative analysis of carnivoran tarsal evolution. In: *Mammalian Evolutionary Morphology: A Tribute to Frederick S. Szalay*. (eds Sargis E, Dagosto M), pp. 165–194. Dordrecht: Springer.

Ravosa MJ, Noble VE, Hylander WL, et al. (2000) Masticatory stress, orbital orientation and the evolution of the primate postorbital bar. *J Hum Evol* **38**, 667–693.

Revell LJ (2012) phytools: An R package for phylogenetic comparative biology (and other things). *Methods Ecol Evol* **3**, 217–223.

Rohlf J (2002) Geometric morphometrics and phylogeny. In: *Morphology, Shape, and Phylogeny*. (eds MacLeod N, Forey PL), pp. 175–193. London: Taylor & Francis.

Schmitz L, Motani R (2011) Nocturnality in dinosaurs inferred from scleral ring and orbit morphology. *Science* **332**, 705–708.

Sillero-Zubiri C, Hoffmann M, Macdonald DW (eds) (2004) *Canids: Foxes, Wolves, Jackals, and Dogs: Status Survey and Conservation Action Plan*, pp. x + -430. Gland: IUCN.

Simons EL (2009) Convergence and frontation in fayum anthropoid orbits. In: *Primate Craniofacial Function and Biology*. (eds Vinyard C, Ravosa MJ, Wall C), Chapter 18, pp. 407–429. Boston: Springer.

Slater GJ, Van Valkenburgh B (2008) Long in the tooth: evolution of sabertooth cat cranial shape. *Paleobiology* **34**, 403–419.

Van Valkenburgh B (1990) Skeletal and dental predictors of body mass in carnivores. In: *Body Size in Mammalian Paleobiology: Estimation and Biological Implications*. (eds Damuth J, McFadden B), pp. 1–205. Cambridge, UK: Cambridge University Press.

Walls GL (1942) The vertebrate eye and its adaptive radiation. *Cranbrook Inst Sci Bull* **9**, 1–785.

Wesley-Hunt GD, Flynn JJ (2005) Phylogeny of the Carnivora: basal relationships among the carnivoramorphans, and assessment of the position of 'Miacoidea' relative to Carnivora. *J Syst Paleontol* **3**, 1–28.

Wilson DE, Mittermeier RA (2009) *Handbook of the Mammals of the World* (No. C/599.012 H3).